Modeling the Dynamics of Cardiac Action Potentials

Graham Duckett and Dwight Barkley*
Mathematics Institute, University of Warwick,
Coventry CV4 7AL, United Kingdom
(Received 2 August 1999)

The nonlinear dynamics of cardiac action potentials is explained via simple model equations describing the membrane potential and the inward and outward currents through the membrane. The equations approximate ionic models, yet are expressed as polynomial functions, and robustly capture the phase-space dynamics of action potentials.

PACS numbers: 87.19.Hh, 05.45.–a, 87.10.+e

Action potentials are the characteristic time series observed in the electrical potential across the membrane of a cardiac or nerve cell following depolarization (firing). While action potentials vary significantly from cell type to cell type [1,2], a typical example for a cardiac cell, obtained from an ionic model [3,4], is shown in Fig. 1(a), together with the associated inward and outward currents through the cell membrane [Fig. 1(b)]. The dynamics of the membrane potential and associated currents are extremely important because these dictate wave propagation in extended physiological media, and in the case of cardiac tissue, these waves are believed responsible for certain arrhythmias, often leading to death [5].

Detailed ionic models are immensely complicated, making analytical treatment impossible and simulations costly (and currently impossible in three dimensions). For this reason, the FitzHugh-Nagumo model [6] has been popular in theoretical and computational studies, e.g., Ref. [7]. The model has just two variables and a cubic nonlinearity. It nevertheless captures the most basic features of action potentials and its simple phase portrait with N-shaped nullcline explains key aspects of excitability. However, the standard FitzHugh-Nagumo model fails to capture the form of fast response action potentials in real cardiac tissue where the time scales of depolarization and repolarization are significantly different, and where early partial repolarization generally follows the upstroke [Fig. 1(a)]. Furthermore, the propagation of wave trains in the FitzHugh-Nagumo model is qualitatively at odds with what is found in cardiac tissue (Fig. 2) where restitution is strong, promoting instability at small diastolic interval [8–10], and dispersion is weak, with wave speed insensitive to the postrepolarization state of the medium.

Models have been proposed to improve the fidelity of the FitzHugh-Nagumo equations while not resorting to full physiological modeling. Of particular importance are models that attempt to capture the restitution and dispersion of cardiac tissue, either through modification of the FitzHugh-Nagumo equations [11,12] or through characterizing basic ionic mechanisms [13]. However, as far as we are aware, there is no published simple model that accurately captures the characteristic action potential and currents shown in Figs. 1(a) and 1(b), and provides explanation for these dynamics.

Here we propose a surprisingly simple approach to understanding and modeling action potentials. Analysis is based on the currents through the cell membrane rather than on the gating mechanisms responsible for these currents. This allows model differential equations to be constructed in terms of low-order polynomials that correctly account for all of the important phase-space features found in ionic models and thus reproduce in detail the dynamics of these complex equations.

Noble's modification [3] of the Hodgkin-Huxley equations [14] produces action potentials and membrane currents (shown in Fig. 1) close to those observed experimentally, and yet for an ionic model it contains few variables. Thus we shall use it as the starting point for developing simple polynomial approximations. The Noble model is

$$\begin{aligned} \dot{\tilde{V}} &= -(\tilde{I}_i + \tilde{I}_o)/C_m\,, \\ \tilde{I}_i &= (400m^3h + \overline{g}_{Na})(\tilde{V} - 40)\,, \\ \tilde{I}_o &= [g_{K_1}(\tilde{V}) + 1.2n^4](\tilde{V} + 100)\,, \\ \dot{y} &= [y_\infty(\tilde{V}) - y]/\tau_y(\tilde{V}) \quad \text{where } y = m, h, n\,, \end{aligned} \tag{1}$$

with dynamical variables $\tilde{V}$ (membrane potential), and m, h, and n (gate variables). C_m is the membrane capacitance.

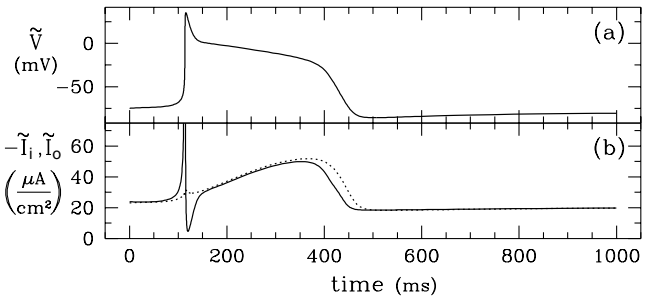

FIG. 1. (a) Typical action potential and (b) corresponding inward (solid) and outward (dotted) membrane currents from the Noble model.

 0031-9007/00/85(4)/884(4)$15.00

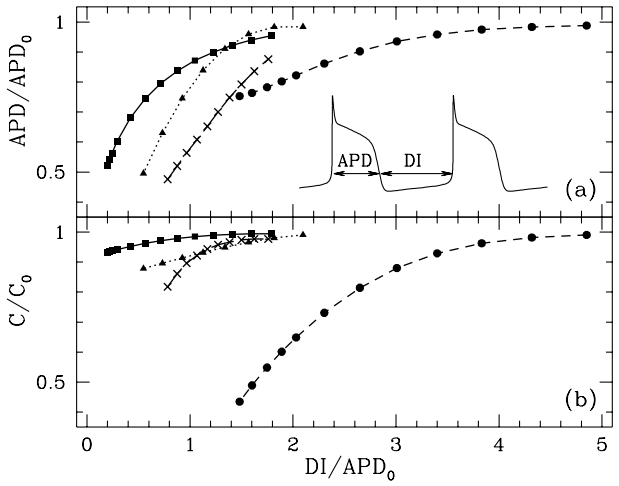

FIG. 2. (a) Restitution and (b) dispersion for the Noble model (squares), the FitzHugh-Nagumo model (circles), model (3) (crosses), and model (4) (triangles). Plotted are the normalized action potential duration APD and wave speed C versus the normalized diastolic interval DI. APD_0 and C_0 are the action potential duration and speed of an isolated pulse (DI $= \infty$).

All functions of $\tilde{V}$, e.g., $m_\infty(\tilde{V})$, are rational functions of exponentials. We use $\tilde{I}_i$ and $\tilde{I}_o$ to denote the inward and outward currents to emphasize that, while originally assumed to be due to sodium and potassium ions only, in reality many other ions participate [15] and only the total inward and outward currents are captured by this model [1]. In particular, the total inward current is primarily due to sodium and calcium currents. In the following we shall indicate parenthetically the roles of the sodium, calcium, and potassium currents.

We write Eqs. (1) in a form useful for subsequent analysis. We adiabatically eliminate the variable m in terms of the voltage-dependent equilibrium $m_\infty(\tilde{V})$, which is a monotonic function of $\tilde{V}$. This is possible since the time scale of the (sodium activation) gate m is at least an order of magnitude faster than any other time scale in the system [1,2]. Simulations show that only small quantitative effects result from the elimination of m [9,16]. We then perform a straightforward change of variables from V, h, and n to V, $\tilde{I}_i$, and $\tilde{I}_o$, and obtain

$$\dot{V} = I_1 - I_2\,, \tag{2a}$$

$$\dot{I}_1 = (f_5 I_1 + f_4)(I_1 + f_3) + f_2 I_1 I_2 + f_1 I_2 + f_0\,, \tag{2b}$$

$$\dot{I}_2 = (I_1 - I_2) g_1(V, I_2) + g_0(V, I_2)\,, \tag{2c}$$

where we have defined nondimensional currents $I_1 = -\tilde{I}_i/I^*$ and $I_2 = \tilde{I}_0/I^*$, where $I^* = 125\ \mu\mathrm{A/cm}^2$ for $C_m = 12\ \mu\mathrm{F/cm}^2$. We have also made the voltage nondimensional by $V^* = 16.3$ mV and time by $t^* = 1.57$ msec. The f_i are functions of V only.

Following a detailed analysis [16] of the phase space of Eqs. (2), the dynamics of action potentials can be understood, and, in fact, almost exactly reproduced, by replacing the complicated functions f_i, g_i derived from the Noble model by relatively simple polynomials. Specifically, f_2 can be approximated by zero (a significant reduction in the nonlinearity of the equations), f_0, f_1, and f_4 can be replaced by constants, g_0 can be taken to be a linear function of V only, and f_5 is proportional to V. While these approximations are generally consistent with the forms obtained from Eqs. (1), the source and justification for the approximations are an analysis of their role in generating dynamics.

We consider two model systems. The first is a qualitative model, with at most cubic nonlinearity, capturing the essential fast or slow dynamics of physiological media:

$$\dot{V} = I_1 - I_2\,, \tag{3a}$$

$$\dot{I}_1 = -(VI_1 + 1)I_1 - I_2\,, \tag{3b}$$

$$\dot{I}_2 = \epsilon[(I_1 - I_2)(I_2 - V) + \alpha + V]\,, \tag{3c}$$

where α and ϵ are parameters. A phase portrait and time series from these equations are shown in Fig. 3. The dynamics is oscillatory with periodic action potentials.

From Eq. (3a), the extrema of V occur at points where the currents are equal. The cubic term $-VI_1^2$ in Eq. (3b) is the essential nonlinearity in the model, and modulo constants, this approximates well $f_5 I_1^2$: the dominant term in Eq. (2b) for large I_1. The role of the nonlinear term can be seen in the I_1 nullclines (curves on which $\dot{I}_1 = 0$). For $I_2 = 0$ these are $I_1 = 0$ and $I_1 = -1/V$ (Fig. 3 inset). For nonzero I_2 the nullclines change qualitatively near $I_1 = 0$ and the symmetry $(V, I_1) \to (-V, -I_1)$ in Fig. 3 is broken, but the curve $I_1 = -1/V$ is persistent for large

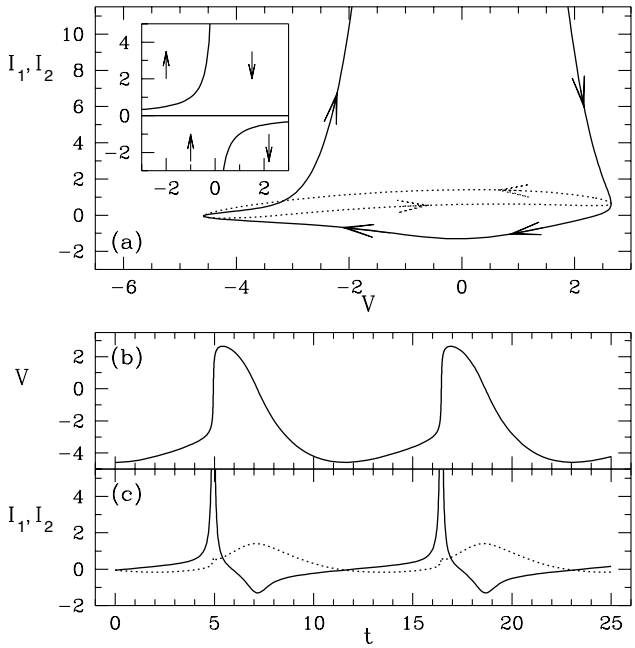

FIG. 3. Dynamics from Eqs. (3) with $\alpha = 3$ and $\epsilon = 0.09$. (a) Phase portrait showing inward current I_1 (solid) and outward current I_2 (dotted) vs V. Inset shows the I_1 nullclines for $I_2 = 0$. Arrows indicate the sign of $\dot{I}_1$. (b) Action potential and (c) currents.

I_1. Approximating $g_1(I_2, V)$ by $\epsilon(I_2 - V)$ in Eq. (3c) is the simplest choice giving correct behavior for I_2 and a reasonable form for the action potentials [17].

Starting from the potential minimum at $t = 0$ (Fig. 3), the dynamics are as follows. The currents balance with I_1 increasing and I_2 decreasing. I_1 is above but near the hyperbolic portion of the nullcline. I_2 reaches a minimum and then increases so that the two currents remain close until $t \simeq 4$, during which time $\dot{V}$ is small. At $t \simeq 4$, I_1 begins to deviate significantly from the nullcline and the term $-VI_1^2 > 0$ leads to explosive nonlinear growth of the inward (sodium) current. This produces the large voltage derivative ($\dot{V} = I_1 - I_2 \gg 1$) of the upstroke. V very quickly becomes positive driving I_1 across its nullcline at a large value ($I_1 \simeq 56$). Then $\dot{I}_1$ changes sign and I_1 rapidly falls. The fast dynamics of the upstroke abruptly ends when $I_1 = I_2$ and V obtains its maximum.

The time scale of repolarization is vastly slower than that of depolarization because the two currents remain close in magnitude. The outward current agrees qualitatively with the outward (potassium) current in physiological media where it plays a dominant role in repolarization. In Eqs. (3) the inward current is not correctly modeled during repolarization (roughly, the effect of the calcium current in cardiac tissue is neglected), and as a result there is no voltage plateau prior to repolarization and the system does not recover to an excitable fixed point. Otherwise, the essential fast (sodium) and slow (potassium) dynamics of physiological media are well captured with a cubic nonlinear model, significantly different from those with N-shaped nullclines as in Fig. 1.

Consider now the quantitative model given by

$$\begin{aligned} \dot{V} &= I_1 - I_2\,, \\ \dot{I}_1 &= -(VI_1 + 1)[I_1 - h_f(V)] + \delta(\beta - I_2)\,, \\ \dot{I}_2 &= \epsilon\{(I_1 - I_2)[I_2 - h_g(V)] + \gamma(\alpha + V)\}\,, \end{aligned} \tag{4}$$

where β, γ, and δ are additional parameters and $h_f(V)$ and $h_g(V)$ are quartic and quadratic polynomials, respectively. The coefficients in $h_f(V)$ and $h_g(V)$ are easily determined by fitting to the nullclines in the Noble equations. For $I_2 = \beta$, the I_1 nullclines are $I_1 = -1/V$ and $I_1 = h_f(V)$ as shown in Fig. 4.

Figure 5 shows time series from this model, and Fig. 6 shows phase portraits for both Eqs. (1) and (4). The dynamics of the two systems are almost identical. For comparison with the Nobel model, and physiological media in general, in Figs. 5 and 6 we plot dimensional variables, $\tilde{V} = VV^*$, $\tilde{I}_1 = I_1 I^*$, $\tilde{I}_2 = I_2 I^*$, and time tt^*.

The nonlinear mechanism of fast depolarization [region 1 of Fig. 6(b)] is as in Eqs. (3). Following the voltage maximum, I_1 falls to nearly zero, and $\dot{V}$ briefly becomes moderately large and negative (region 2). This generates the partial repolarization from the outward (potassium) current generally observed in fast response action potentials [1,2]. There is then a second rise of the inward (calcium [1,2]) current as I_1 follows the quartic branch

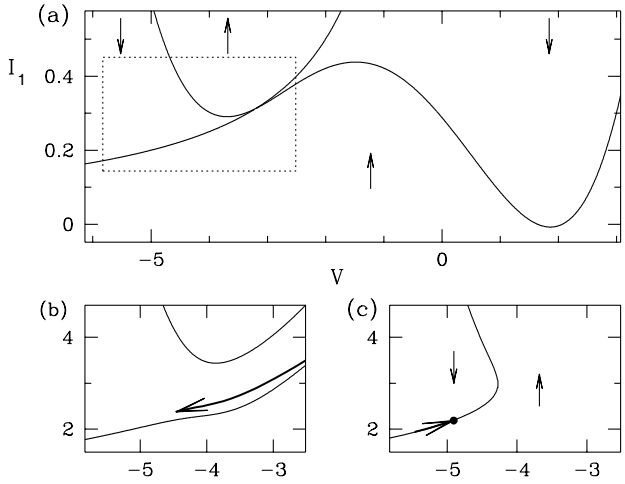

FIG. 4. (a) I_1 nullclines with $I_2 = \beta$ for Eqs. (4). (b) $I_2 > \beta$: nullcline crossing in (a) breaks to form channel for I_1 trajectory (bold). (c) $I_2 < \beta$: nullcline crossing breaks in other direction generating an excitation threshold for fixed point (dot).

of the nullcline (region 3). [Heuristically, the dynamics of the calcium component of the inward current results from the nullcline $I_1 = h_f(V)$.] The voltage plateau occurs because a near balance of current is established. Both currents increase slowly ($\dot{I}_2$ is small because $I_1 - I_2$ is small, and hence γ dictates the length of the plateau). Once I_1 reaches the local maximum of its nullcline it again decreases, increasing $|\dot{V}|$ and leading to repolarization (region 4).

The final recovery of the system and establishment of a voltage threshold for reexcitation is shown in Figs. 4(b) and 4(c). With $I_2 > \beta$ the nullclines form a channel for the I_1 trajectory. The system is absolutely refractory because no voltage perturbation can put the system above the upper nullcline in Fig. 4(b) and reexcite the system. (Note that $I_2 > \beta = 0.3$ corresponds to $\tilde{I}_2 > \beta I^* = 37.5\ \mu\mathrm{A/cm}^2$.) After I_2 falls below the value β, the nullclines change qualitatively establishing a voltage threshold for excitation.

We have simulated wave trains in one dimension and spiral waves in two dimensions using both current models

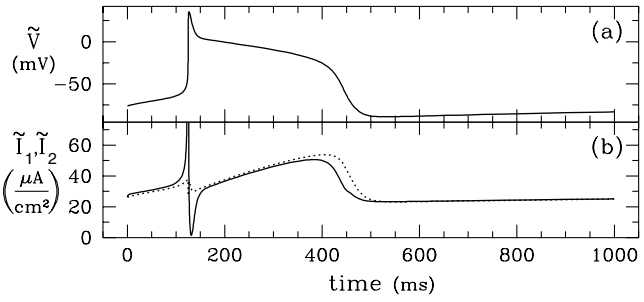

FIG. 5. (a) Action potential and (b) membrane currents from Eqs. (4) shown in dimensional variables. Parameters are $\alpha = 4.9$, $\beta = 0.3$, $\gamma = 8 \times 10^{-4}$, $\delta = 0.12$, $\epsilon = 0.33$; $h_g(V) = -0.0333(V + 1.23)^2 + 0.365$ and $h_f(V) = 4.65 \times 10^{-3}V^4 + 0.0205V^3 - 0.0384V^2 - 0.188V + 0.288$.

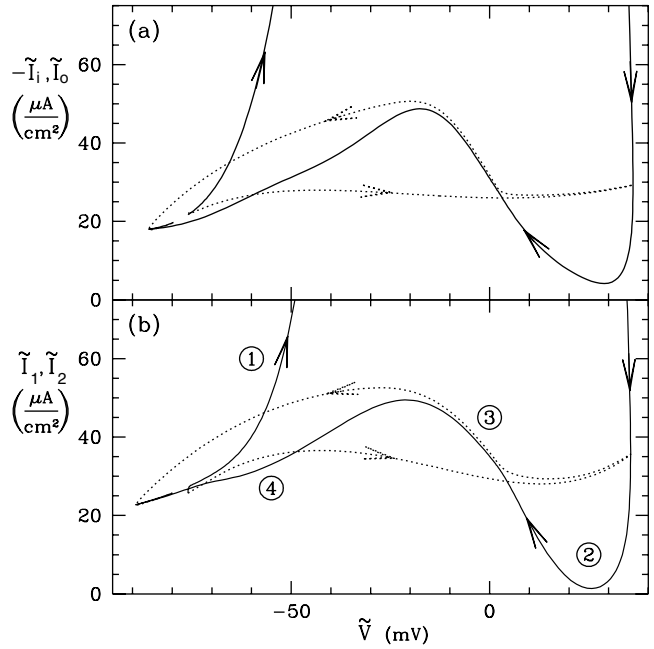

FIG. 6. Trajectories of inward (solid) and outward (dotted) currents vs voltage for (a) the Noble model and (b) Eqs. (4). Both systems are excitable: trajectories start from $\tilde{V} = -76$ and eventually return to fixed points with $\tilde{V} \simeq -80$. See text for explanation of the four regions in (b).

(3) and (4) by including spatial variation in the membrane potential and currents [18]. The normalized restitution and dispersion curves for both current models are qualitatively of the type observed in cardiac tissue (Fig. 2). These curves are for the same parameters as are used in homogeneous simulations in Figs. 3 and 5; however, for model (4) using $\delta = 0.3$ gives waves with action potentials more like those in cardiac tissue. The evolution to spiral waves starting from broken wave fronts in both current models is very similar to that found in the Noble model. With suitable choice of arbitrary length and time scales, the period, wavelength, and core size of spirals based on Eqs. (3) agree with spirals in the Noble model. The spiral period based on Eqs. (4) is 45 ms compared with 65 ms for the Noble model using parameters in this paper. However, the spiral wavelength and core size from Eqs. (4) are both approximately a factor of 3 smaller than those in the Noble model. The reason for this difference is currently not understood.

We have demonstrated an approach to modeling cardiac action potentials using a small number of physiologically relevant variables whose phase-space dynamics can be precisely understood. On the one hand, Eqs. (3) elucidate the essential nonlinear dynamics of all fast response action potentials and have significant advantages over N-shaped-nullcline models such as the FitzHugh-Nagumo model. On the other hand, Eqs. (4) demonstrate how this approach can be used to reproduce and understand detailed dynamics of realistic action potentials using relatively simple equations. By varying the parameter values and functions h_f and h_g in Eqs. (4), it is possible to capture, at least qualitatively, many types of action potentials observed in physiological media [16]. Finally, work is ongoing using four-dimensional models with independent sodium and calcium currents. While desirable from a physiological perspective, this extension diminishes the simplicity of phase-space analysis reported here and will be presented elsewhere.

This work has been supported in part by the EPSRC (Grant No. GR/K88118).

*Email address: barkley@maths.warwick.ac.uk

[1] D. Noble, *The Initiation of the Heartbeat* (Oxford University Press, Oxford, 1979), 2nd ed.
[2] R. M. Berne and M. N. Levy, *Cardiovascular Physiology* (Mosby-Year Book, Inc., St. Louis, 1992).
[3] D. Noble, J. Physiol. **160**, 317 (1962).
[4] A. V. Panfilov and A. V. Holden, Int. J. Bifurcation Chaos Appl. Sci. Eng. **1**, 219 (1991).
[5] The most recent review can be found in Chaos **8** (1998).
[6] R. FitzHugh, Biophys. J. **1**, 445 (1961); J. S. Nagumo, S. Arimoto, and S. Yoshizawa, Proc. IRE **50**, 2061 (1962).
[7] A. Winfree, Chaos **1**, 303 (1991); A. Karma, Phys. Rev. Lett. **68**, 397 (1992); D. A. Kessler, H. Levine, and W. N. Reynolds, Phys. Rev. Lett. **68**, 401 (1992); D. Barkley, Phys. Rev. Lett. **72**, 164 (1994).
[8] G. R. Mines, J. Physiol. (London) **46**, 349 (1913); J. B. Nolasco and R. W. Dahlen, J. Appl. Physiol. **25**, 191 (1968); M. R. Guevara, G. Ward, A. Shrier, and L. Glass, in *Computers in Cardiology* (IEEE Computer Society Press, Salt Lake City, 1984), p. 167; M. Courtemanche, L. Glass, and J. P. Keener, Phys. Rev. Lett. **70**, 2182 (1993).
[9] A. Karma, Phys. Rev. Lett. **71**, 1103 (1993).
[10] A. Karma, Chaos **4**, 461 (1994).
[11] R. R. Aliev and A. V. Panfilov, Chaos Solitons Fractals **7**, 293 (1996).
[12] B. Y. Kogan *et al.,* Physica (Amsterdam) **50D**, 327 (1991).
[13] F. Fenton and A. Karma, Chaos **8**, 20 (1998).
[14] A. L. Hodgkin and A. F. Huxley, J. Physiol. **117**, 500 (1952).
[15] R. E. McAllister, D. Noble, and R. W. Tsien, J. Physiol. **251**, 1 (1975); G. W. Beeler and H. Reuter, J. Physiol. **268**, 177 (1977); D. DiFrancesco and D. Noble, Philos. Trans. R. Soc. London B **307**, 353 (1985); Ch. Luo and Y. Rudy, Circ. Res. **68**, 1501 (1991); **74**, 1071 (1994).
[16] G. Duckett (to be published).
[17] The simpler approximation $g_1 = \epsilon$ results in a model with a single nonlinear term, but gives poorer approximation to action potentials.
[18] Including spatial variation introduces the Laplacian of voltage into both the V and also the current equations. See [16] for details.